For office use only	Team Control Number	For office use only
T1 _____	**84486**	F1 _____
T2 _____		F2 _____
T3 _____	Problem Chosen	F3 _____
T4 _____	**A**	F4 _____

2019
MCM/ICM
Summary Sheet

(Your team's summary should be included as the first page of your electronic submission.)
Type a summary of your results on this page. Do not include the name of your school, advisor, or team members on this page.

Summary

In order to analyze the propagation process of HF skywave, especially the reflection off the ocean surface and different terrains, this paper proposed a model including the modeling of different reflecting surfaces and discussions about different modes of reflection. Essentially, the model is established on the theory of *Geometrical Optics* and *Statistics*.

When the reflection takes place on the ocean surface, we specify that the ocean state is either *Calm* or *Turbulent*. For the calm ocean, we suppose the surface to be smooth enough for specular reflection, and that the reflective signal direction obeys the law of reflection. The strength of the signal is determined by the reflectance at the incident point, which correlates to the incident angle strongly, according to Fresnel equation. For the turbulent one, the mode of reflection remains the same, but the reflecting surface is quite different. We simulate the turbulent ocean surface with the method of linear filtering, and with reference to the JONSWAP sea spectra. Then we are able to work out the normal vector to calculate the direction of reflective signal as well as the strength.

We apply *statistical analysis of the signal histogram* to the reflections off the ocean surface, especially turbulent surface, attempting to have a novel view on this problem (signal histogram here refers to a histogram that contains the information of both the strength and the direction of the signal). When trying to meet the communication demand of a shipboard receiver moving on a turbulent ocean, we indeed have some discoveries about the choice of the optimal heading for the ship.

Eagering to go further with statistical methods, we boldly assume that the reflections off rugged terrain features *Lambertian Reflection*. Then we take a mesoscale look at the topological inequalities, which enables us to ignore the detailed shape information, and focus on their heights and the distance between them. We intuitively assume distance yields a *Uniform Distribution*, while the height has a *Gaussian Distribution*, and manage to statistically work out the strength of the reflective signal.

Observing that the model fits in some certain cases well, we suggest that such an attempt to apply statistical method is worthwhile.

Keywords: Geometrical Optics; Fresnel equation; Linear filtering; JONSWAP sea spectra; Statistical Method; Lambertian Reflection; Gaussian Distribution; Uniform Distribution; Histogram Analysis

An attempt to apply the statistical method to HF wave propagation

During the recent decades, we have witnessed a rapid and revolutionary growth in the field of radio propagation. Massive numerical algorithms have been developed to analyze and clarify the propagation mode, and phenomena of reflection, refraction, diffraction, absorption, polarization, and scattering are adequately discussed from the view of electromagnetic radiation. We would like to introduce our attempt to apply the statistical method to HF wave propagation briefly in this paper.

We focus exclusively on the reflections off the turbulent ocean surface as well as the rugged terrain, considering the complexity of these circumstances, together with the curiosity about the performance of statistical tools in such a kind of problem.

We assume that the signal propagates in terms of ray, and obeys the law of reflection. Also, it satisfies the condition of Fresnel equation, which enables us to get a approximate estimation of its strength. We suggest that on both the smooth terrain and calm ocean, the pattern of reflection can be easily described by reflectance, varying with the incident angle and the electromagnetic constants (Figure 1).

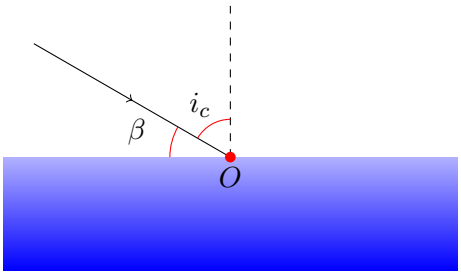

Figure 1: Specular Reflection

For the rugged terrain, we boldly assume that the reflections features *Lambertian Reflection*. Then we ignore the detailed shape of the topographic inequalities, and pay extra attention to the heights and the distance between each pair of them (Figure 2). We intuitively assume distance yields a *Uniform Distribution*, while the height has a *Gaussian Distribution*, and manage to statistically work out the strength of the reflective signal that varies with the terrain.

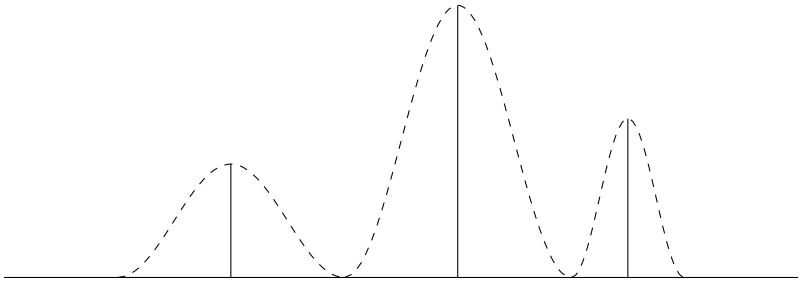

Figure 2: The Abstract of Topographic Inequalities

In addition, we considered the communication problem for ships traveling across the turbulent ocean, and managed to apply the statistical analysis of signal histogram to work out the optimal direction for shipboard receiver to receive the signal. In our methodology, scatter graph such as Figure 3a, indicates the distribution of both the propagation direction and

the strength. The variation of colors demonstrates the difference of strength. Histogram such as Figure 3b, points out the optimal direction where we are most likely to meet the strongest signal.

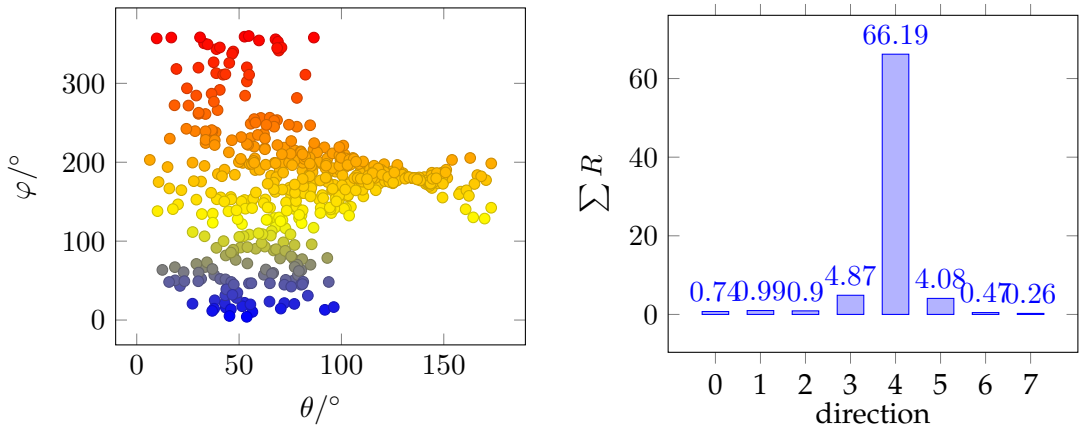

(a) Scatter graph of the distribution of θ and φ

(b) Histogram of total reflectance in each direction

Figure 3: Distribution of the reflective signal

Finally, we would like to thank all of those who have made significant contributions to this field, including the contributing authors, the anonymous reviewers, and the IEEE Communications Magazine publications staff, in particular the Editor-in-Chief. We believe that the research results presented in this Feature Topic will further stimulate research and development ideas in HF wave propagation.

An attempt to apply the statistical method to HF wave propagation & communication

January 31, 2019

Contents

1 Introduction

1.1 Clarification of the problem

Radio waves with high frequency (HF, defined to be 3-30 MHz), ideally, can travel across continents, due to the existence of ionosphere and the multiple reflections off it. Yet the strength of the signal attenuates in each turn of the propagation direction. Among other factors, the characteristics of the reflecting surface dominate the strength of the reflected wave and how far the signal can ultimately travel, while the utility is still acceptable.

We are required to analyze, mainly the signal strength and propagation direction, of reflections with the reflecting surface varying from calm ocean surface to rugged terrain. In this problem, we focus exclusively on the reflections off the turbulent ocean surface as well as the rugged terrain, considering the complexity of these circumstances. The reflection off ionosphere is also referred to. We attempt to clarify how the incident angle, and the roughness of the reflecting surface affects the reflection.

By synthesizing the geometrical optics and statistical tools, we manage to model the propagation process of HF sky-wave signal, and tackle the strength variation and direction distribution during the process with care and simplicity.

1.2 Principles of our Model

The model we present in this paper can be divided into two parts, one for ocean reflection and one to model the terrain reflection considering the diffuse reflection.

Our reflection model for ocean essentially bases on the Fresnel equation, and we apply the JONSWAP sea spectra to fit in the function of wave spectrum with the method of linear filtering, which enables us to simulate the turbulent ocean surface. With the knowledge of surface function f, we can calculate the normal vector at the incident point, and thus determine the propagation direction of the signal as well as the strength.

With statical analysis of signal histogram, which contains the information of both strength and direction, introduced, we developed an original model to accommodate the shipboard receiver moving on a turbulent ocean. The model manages to indicate the optimal direction for the receiver, and helps to figure out how long the ship can remain in communication depending on its heading.

The reflection model for terrain, especially the rugged terrain, is based on the Lambertian Reflection and an abstraction that ignores the detailed shape of the topographic inequality. We apply *Gaussian Distribution* to the height and *Uniform Distribution* to the distance between any pair of the topographic inequalities, and thus statistically generate the strength of the signal.

1.3 Underlying Assumptions & Notation

- The reflection of the radio waves is considered within the scope of Geometrical Optics.
- Seawater and the air can be regarded as non-magnetic media.
- At the point at which reflection occurs, the incident signal is assumed to be plane wave and effects of edges are neglected. The interface between seawater and the air is flat and that the media are homogeneous. Under such conditions, the reflection can be described by Fresnel equation.

- Radio waves are generally polarized. In this problem, we assume that radio waves are circularly polarized.
- We assume that launching angle of the radio is more than 50°. This is reasonable in long-distance propagation.
- In rough terrain, heights and distances of topographic inequalities are crucial factors that influence the reflection. We ignore the detailed shape for simplicity.
- The surface of the mountain meets the characteristics of *Lambertian Reflection*, and the reflection of radio waves in the mountain area follows the law of ideal diffuse reflection.
- The speed of the ship remains unchanged.
- The height of the shipboard receiver relative to the ship is fixed. And we assume that sea waves will not strongly influence the height of the receiver.

Table 1: Notation(Variables)

Symbol	Definition	Units
L	The launch point of the radio on land	
O	The receive point on the ocean surface, which is also the origin of the coordinate on the ocean	
M	The point on the ionosphere where the radio hit	
C	Central point of earth	
P	A certain point on the turbulent Ocean	
β	Launching angle of the radio	rad
i_{t}	Incident angle on turbulent ocean	rad
i_{c}	Incident angle on calm ocean	rad
φ	The phase of the radio signal	rad
I_0	The strength of radio from the source	Watt
I_1	The radio strength after the first reflection off the ionosphere	Watt
$I_{2,\mathrm{c}}$	The radio strength after the first reflection off the calm sea	Watt
$I_{2,\mathrm{t}}$	The radio strength after the first reflection off the turbulence sea	Watt
$I_{t,\mathrm{s}}$	The radio strength after the reflection off the smooth terrain	Watt
$I_{t,\mathrm{r}}$	The radio strength after the reflection off the rugged terrain	Watt
b	The average carrier power	Watt
b_1	The average carrier power after the first reflection off the ionosphere	Watt
T	The temperature of seawater	°C
S	The salinity of seawater	ppt
R_c	The reflectance of calm ocean	
R_t	The reflectance of turbulent ocean	
R	The reflectance	
k	The proportionality constant between the strength of the signal and square of the amplitude	
α	the percentage of signal that will be reflected off the pair and continue to propagate	
N_m	The maximum number of hops	
D	Max communication distance	m
t	Max communication time	s

Table 2: Notation(Constants)

Symbol	Definition	Value
H	The height of the ship	30 m
s	The speed of the ship	10 m/s
g	Gravity acceleration	9.8 m/s^2
b_0	The carrier power of the signal which is transmitted	100 W
SNR	Usable signal-to-noise ratio	10 dB
n_1	Refractive index of air	1.00

2 Reflection off the ionosphere

Before its encounter with the ocean, HF signal will have to suffer from *Rayleigh Fading*[1] first, during the reflection off the ionosphere.

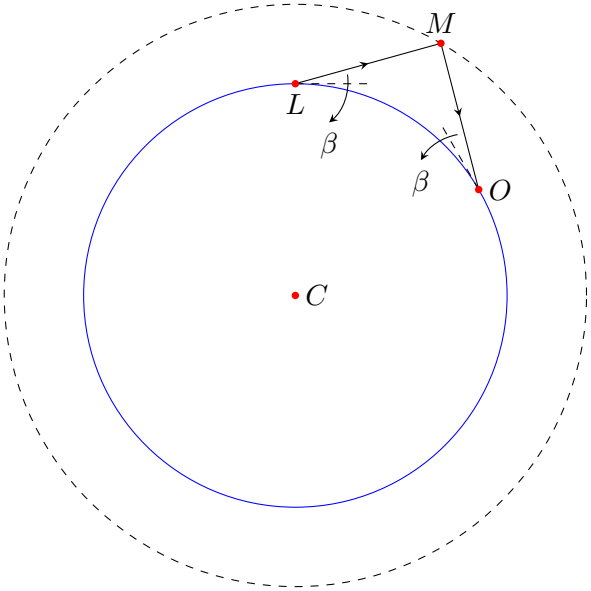

Figure 1: Reflection off ionosphere

By applying *Rayleigh Distribution* to the amplitude distribution, we get a probability density function of the decayed amplitude:

$$p_R(A) = \frac{A}{b} \mathrm{e}^{-\frac{A^2}{2b}} \tag{2.1}$$

where b is the average carrier power and A refers to the amplitude.

According to electromagnetic theory, the strength of the radio is proportional to the square of the amplitude. The proportionality constant is denoted by k:

$$I = kA^2 \tag{2.2}$$

With equation (2.1), we are able to calculate the expectation of the strength:

$$\begin{aligned} I_1 &= k \int_0^{+\infty} A^2 p_r(A)\,\mathrm{d}r \\ &= k\sqrt{2b\pi} \end{aligned} \tag{2.3}$$

3 Reflection off a Moody Ocean

3.1 Setting up the Coordinate System

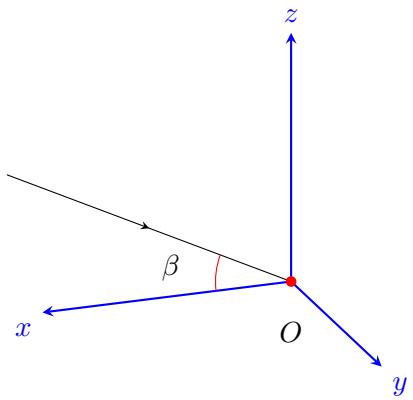

Figure 2: The Coordinates

For simplicity's sake, we omit other complicated, trivial hypotheses but decrease amplitude of the signal when depicting the reflection off the ocean. We also set up a rectangular coordinate system (Figure 2), which takes the Point O (Figure 1 ,2) as its origin, as well as LMO in its xOz plane.

3.2 Simulating the Ocean Surface

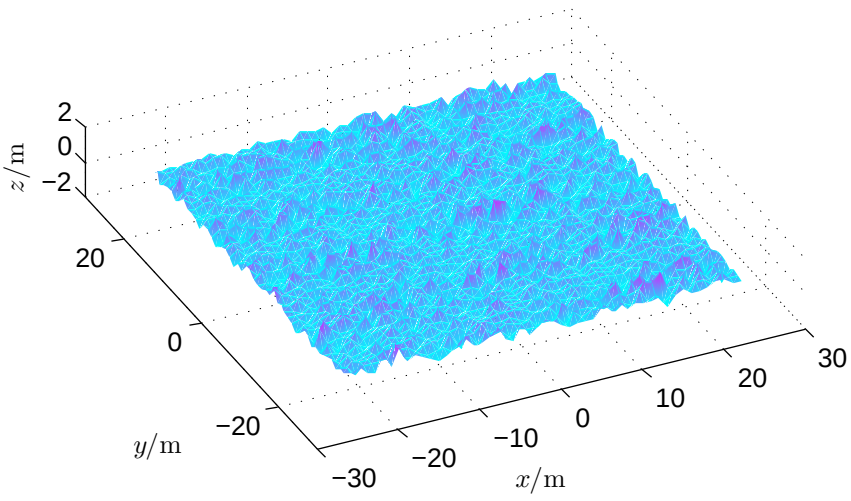

Figure 3: Simulation of Ocean Surface

Here we apply the method of linear filtering, which enables us to simulate the surface of a turbulent ocean[2]. The ocean surface is a small rectangular region (Figure 3), denoted by $L_x \times L_y$, where both L_x and L_y are sets of points. The number of discrete points on x and y axes are M and N, which, in practice, has a positive correlation with the smoothness level of the surface.

The height of each single point $P(x_m, y_n)$ on the wave can be described by the following function:

$$f(x_m, y_n) = \frac{1}{L_x L_y} \sum_{m_l=-\frac{M}{2}+1}^{\frac{M}{2}} \sum_{n_l=-\frac{N}{2}+1}^{\frac{N}{2}} F(k_{m_l}, k_{n_l}) \cdot e^{\mathrm{i}(k_{m_l} x_m + k_{n_l} y_n)} \tag{3.1}$$

where

$$F(k_{m_l}, k_{n_l}) = 2\pi [L_x L_y S(k_{m_l}, k_{n_l})]^{1/2} \times e^{\mathrm{i}\omega_{m_l,n_l} t} \cdot N(0,1) \tag{3.2}$$

To fit in the function of wave spectrum $S(k_{m_l}, k_{n_l})$, we adopt the JONSWAP sea spectra (See more in Appendix A). The simulation results are shown in Figure 3.

3.3 Addressing the Reflectance

As the signal reaches the ocean surface, only part of it reflects again back to the ionosphere, aiming for the next hop, while the other part dives straight in the ocean. The proportion of each part is described appropriately in terms of radiant flux, which is known as *Reflectance*. To calculate the reflectance, we carefully choose the *Fresnel equations*[3]. For non-magnetic media ($\mu_1 \approx \mu_2 \approx \mu_0$):

$$R_{\mathrm{s}} = \left| \frac{n_1 \cos i - n_2 \sqrt{1 - \left(\frac{n_1}{n_2} \sin i\right)^2}}{n_1 \cos i + n_2 \sqrt{1 - \left(\frac{n_1}{n_2} \sin i\right)^2}} \right|^2 \tag{3.3}$$

and

$$R_{\mathrm{p}} = \left| \frac{n_1 \sqrt{1 - \left(\frac{n_1}{n_2} \sin i\right)^2} - n_2 \cos i}{n_1 \sqrt{1 - \left(\frac{n_1}{n_2} \sin i\right)^2} + n_2 \cos i} \right|^2 \tag{3.4}$$

where R_s and R_p refers respectively to the reflectance of s-polarized and p-polarized light.

Thus, due to our assumption that seawater and the air can be approximately regarded as non-magnetic media, the reflectance is:

$$R = \frac{I_{\mathrm{r}}}{I_1} = \frac{I_{\mathrm{r,s}} + I_{\mathrm{r,p}}}{I_1} = \frac{R_{\mathrm{s}} I_{1,\mathrm{s}} + R_{\mathrm{p}} I_{0,\mathrm{p}}}{I_1} \tag{3.5}$$

Usually the radio wave is polarized, and here we adopt the assumption that the radio wave is circularly polarized, which means $I_{1,\mathrm{s}} = I_{1,\mathrm{p}} = I_0/2$. Then we get

$$R = \frac{R_{\mathrm{s}} + R_{\mathrm{p}}}{2} \tag{3.6}$$

3.4 Rectifying the Permittivity

Realizing that the local permittivity of the ocean is, to some extent, decided by its temperature and salinity, we employ the Debye function[4]:

$$\varepsilon(S,T,\omega) = \varepsilon_\infty(S,T) + \frac{\varepsilon_1(S,T) - \varepsilon_\infty}{1 - \mathrm{i}\omega(S,T)} - \frac{\mathrm{i}\sigma(S,T)}{\omega\varepsilon_0} \tag{3.7}$$

where $\varepsilon_0 = 8.854 \times 10^{-12}\mathrm{F/m}$ is the free space dielectric constant; S, T denote the salinity and temperature of seawater; Conductivity σ; Static dielectric constant ε_1 and relaxation time τ varies with T and S

$$\begin{aligned}\varepsilon_1(S,T) =& (87.134 - 0.1949T - 0.01276T^2 + 0.000249T^3) \cdot \\ & (1.0 + 1.1613 \times 10^{-5}TS - 7.638 \times 10^{-4}S - \\ & 7.760 \times 10^{-6}S^2 + 1.105 \times 10^{-8}S^3)\end{aligned} \tag{3.8}$$

In this problem, we assume S and T yields a *Uniform Distribution*, and S is in the range of $[25, 35]$, and T varies from 15 to 25[5].

3.5 When it's Calm

Mirror-like ocean surface can always be delightful.

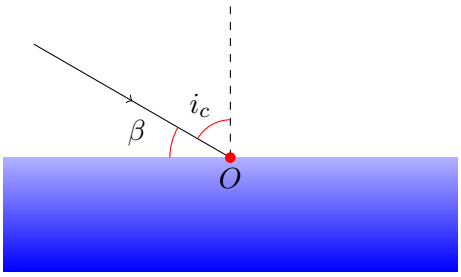

Figure 4: Calm Ocean

It's much easier to apply the metric of Reflectance under this circumstance, compared with the following case. With the knowledge of the incident angle, co-angle of β (in 1), we can get the reflectance directly by Formula(3.3)(3.4)(3.6):

$$I_{2,\mathrm{c}} = RI_1 \tag{3.9}$$

When simulating, we set both S and T (Section 3.4) to be the expectation of their distribution separately.

3.6 Multiple-hop Propagation across the Calm Ocean

Taking the spherical symmetry of the reflecting surfaces(both the ocean surface and ionosphere, Figure 1) into consideration, we realize that the first reflection off the calm ocean makes a basic step to calculate the maximum number of hops. More specifically, because of the invariability of the incident angle on the ocean and on the ionosphere, each hop can be regarded

as a repetition of the first reflection off the calm ocean, simply by taking the reflected signal in the previous hop as the input signal of the next hop. In short, we iteratively conduct the process in section 3.5 until the strength falls below SNR threshold.

Thus, after calculating the $I_{2,c}$, we managed to obtain a coefficient which reveals the decaying rate of the strength of the signal, denoted by d_c:

$$d_c = \frac{I_{2,c}}{I_0} \tag{3.10}$$

Then, during the iteration, the strength of the signal is:

$$I_{N,c} = d_c^N I_0 \tag{3.11}$$

where N refers to the number of iteration. Hence, the maximum number of hops the signal can take is:

$$N_m = \frac{\ln \frac{I_{\text{noise}}}{I_0} + 10}{\ln d_c} \tag{3.12}$$

3.7 How to cope with a Turbulent Ocean

Turbulent ocean differs from the calm ocean with its wave heights, shapes change rapidly. Thus to cope with the turbulent ocean is to handle the surface distorted by ocean turbulence, which hinders us from getting the exact incident angle.

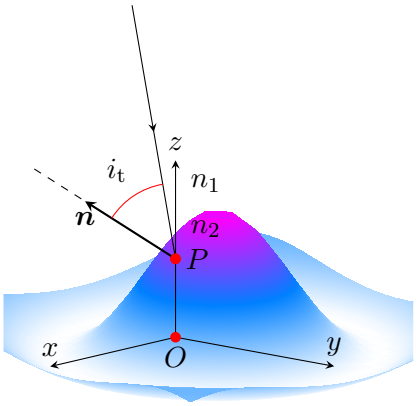

Figure 5: Radio Reflection off a Turbulent Ocean

As is shown above, we build a coordinate system in which the radio path $L \to M \to O$ (Figure 1) locates in the xOz plane to simplify the analysis. $P(x, y, z)$ in Figure 5 represents incident point and the normal vector refers to $\boldsymbol{n}(n_x, n_y, n_z)$, which can be calculated with the knowledge of (3.1). In this case, the reflection doesn't take place at the origin. Instead, we assume that P is right above O.

In the designed coordinate system, the direction vector of MO can be written as:

$$\boldsymbol{l} = (\cos\beta, 0, \sin\beta) \tag{3.13}$$

Then we can easily get the incident angle i from $\boldsymbol{n}$ and $\boldsymbol{r}$:

$$i = \arccos\left(\frac{\boldsymbol{n}\cdot\boldsymbol{l}}{|\boldsymbol{n}|\cdot|\boldsymbol{l}|}\right) = \arccos\left(\frac{n_x\cos\beta + n_z\sin\beta}{\sqrt{n_x^2+n_y^2+n_z^2}}\right) \tag{3.14}$$

With incident angle i, we can work out the reflectance of s-polarized light and p-polarized light by conducting Formula(3.3)(3.4)(3.6). And thus we get:

$$I_{2,\mathrm{t}} = RI_1 \tag{3.15}$$

Considering the waves in a turbulent ocean change rapidly, we let S be $U(25,35)$ and T be $U(15,25)$ in simulation.

4 Hopping about on land

4.1 Model of Smooth Terrain

For smooth terrain, it features plain. Thus the analysis of smooth terrain closely resembles that of the calm ocean surface (see section 3.5). However, it is necessary to pay some extra attention to the ground electromagnetic constants and roughness of the surface, which largely affect the reflectance of the signal.

As is mentioned above, here we'll apply Formula(3.3)(3.4)(3.6) again, and thus we get:

$$I_{t,\mathrm{s}} = R_{t,\mathrm{s}}I_1 \tag{4.1}$$

where $R_{t,\mathrm{s}}$ refers to the reflectance of the smooth terrain.

4.2 Model of Rugged Terrain

Rugged or mountainous terrain requires more subtlety, so we employ a model in which heights and distances of topographic inequalities are abstracted to be the dominant variables, while the details of shape are ignored (Figure 6). Therefore we construct a discrete distribution of topographic inequalities where the distance between any pair of them yields a *Uniform Distribution*, and the height of topographic inequality has a *Gaussian Distribution*[6].

Considering the roughness of the rugged surface and also, for the sake of simplicity, we assume that the reflecting surface is ideal for diffuse reflection, which is said to exhibit *Lambertian*

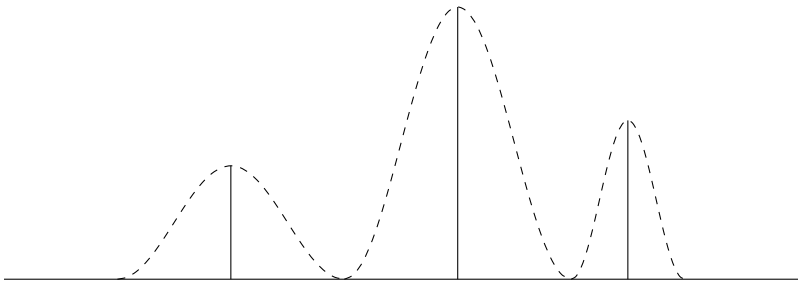

Figure 6: The model of Topographic Inequalities

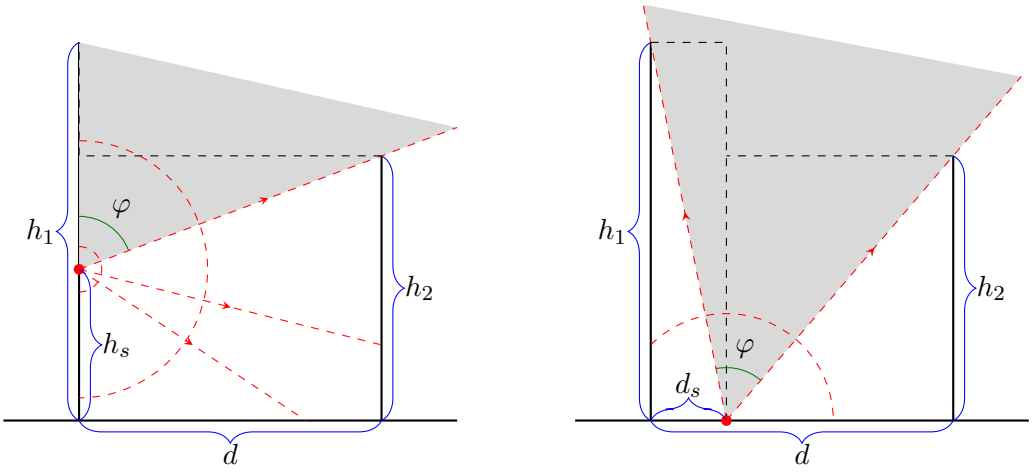

(a) Sub source on the hill (b) Sub source on the ground

Figure 7: Diffuse reflection on the hill

Reflection[7], and we assume that for the same multi-hop path, the reflections will take place in a certain pair of topographic inequalities. The two assumptions indicate that the propagation is established on the *Lambertian Reflection*, which means only the signal that escapes from the pair, denoted by the gray region in Figure 7, can move on, while the rest remains jumping around between the mountains. Naturally, we introduce a ratio α to denote the percentage of signal that will be reflected off the pair and continue to propagate.

Let h_1, h_2 denote the heights of the pair (also the pair itself), and d denote the distance between them. We can easily get the α when the reflection takes place at h_1 (Figure 7):

$$\alpha_{h1}(h_{\mathrm{i},1}) = \frac{1}{\pi} \arctan \frac{d}{h_2 - h_{\mathrm{i},1}} \tag{4.2}$$

where h_{i} denotes the height of the incident point.

Considering the symmetry, we get:

$$\alpha_{h2}(h_{\mathrm{i},2}) = \frac{1}{\pi} \arctan \frac{d}{h_1 - h_{\mathrm{i},2}} \tag{4.3}$$

when the reflection takes place at h_2(Figure 7).

The chances are that the incident point is on the ground, and we use d_{i}(Figure 7) to describe the distance between the point and h_1.

$$\alpha_d(d_{\mathrm{i}}) = \frac{1}{\pi} \left(\arctan \frac{d_{\mathrm{i}}}{h_1} + \arctan \frac{d - d_{\mathrm{i}}}{h_2} \right) \tag{4.4}$$

To take all the possible incident points into account, we calculate the expectation for $\alpha_{h1}(h_{\mathrm{i},1})$ (with the assumption that the height of incident point yields a *Uniform Distribution*):

$$E(\alpha_{h1}) = \frac{1}{h_1} \int_0^{h1} \alpha_{h1}(h_{\mathrm{i},1}) \, \mathrm{d}h_{\mathrm{i},1} \tag{4.5}$$

Using the integral formula in appendix B, we get:

$$
\begin{aligned}
E(\alpha_{h1}) =& \frac{1}{\pi h_1}\left(-\frac{1}{2}d\ln(d^2+((h_2-h_1)^2)+h_1\arctan\frac{d}{h_2-h_1}+\right.\\
&\left. h_2\arctan\frac{h_2-h_1}{d}+\frac{1}{2}d\ln(d^2+h_2^2)-h_2\arctan\frac{h_2}{d}\right)
\end{aligned}
\tag{4.6}
$$

Similarly, we get the expectation of α for the other two cases:

$$
\begin{aligned}
E(\alpha_{h2}) =& \frac{1}{\pi h_2}\left(-\frac{1}{2}d\ln(d^2+((h_2-h_1)^2)+h_2\arctan\frac{d}{h_1-h_2}+\right.\\
&\left. h_1\arctan\frac{h_1-h_2}{d}+\frac{1}{2}d\ln(d^2+h_1^2)-h_1\arctan\frac{h_1}{d}\right)
\end{aligned}
\tag{4.7}
$$

$$
\begin{aligned}
E(\alpha_d) =& \frac{1}{\pi d}\left(h_1\ln h1+h_2\ln h_2+d\arctan\frac{d}{h_1}+\right.\\
&\left. d\arctan\frac{d}{h_2}-\frac{h_1}{2}\ln(d^2+h_1^2)-\frac{h_2}{2}\ln(d^2+h_2^2)\right)
\end{aligned}
\tag{4.8}
$$

We reach the final α by applying the weighted average:

$$
\alpha(h_1,h_2,d)=\frac{E(\alpha_{h1})h_1+E(\alpha_{h2})h2+E(\alpha_d)d}{h_1+h_2+d} \tag{4.9}
$$

In practice, we use Monte Carlo method with the (h_1, h_2, d) tuple varying to calculate the statistical global expectation of α using the equations mentioned above.

Our final goal is to work out the signal strength after the intricate reflections off the rugged terrain. To do so, we manage to fit an average reflectance R of the rugged terrain, and consider the strength to be the sum of escaped signal strength:

$$
\begin{aligned}
I_{t,\mathrm{r}} &= \sum_{i=0}^{+\infty}\alpha R I_1 t^i(1-\alpha)^i\\
&= \frac{\alpha R I_1}{1-(1-\alpha)R}
\end{aligned}
\tag{4.10}
$$

The last equation bases on the fact that both α and R are variables in the range of $[0, 1]$.

5 Sticking to the Same Multi-hop Path

Waves in a turbulent ocean change rapidly over time, so the time-dependent function (3.1), which calculates the instantaneous direction of signal propagation, is not a appropriate choice for our model when there is a demand for accommodating a shipboard receiver moving on a turbulent ocean. Our goal is to rid the model of the dependency of time.

Inspired by the theory of *Statistical Analysis of Histogram*, which is widely used in the field of computer vision, we introduce a signal histogram into our model. Now that we have the incident direction $\boldsymbol{l_1}$ and the normal vector $\boldsymbol{n}$ (from the Formula 3.1), we can calculate the direction of the reflective signal $\boldsymbol{l_2}$:

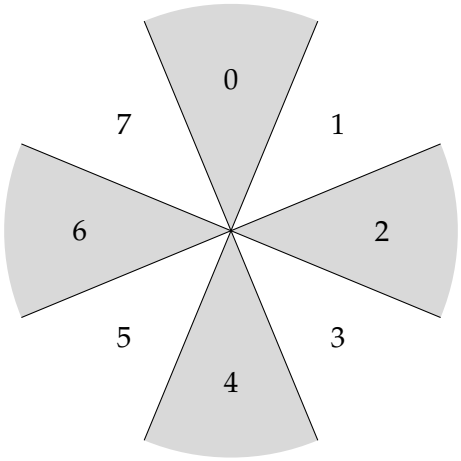

Figure 8: 8 possible directions

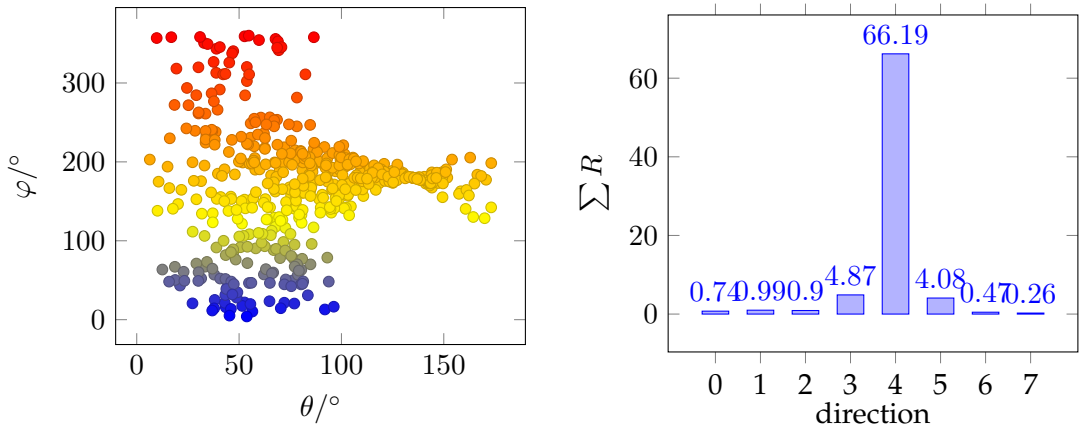

(a) Scatter graph of the distribution of θ and φ

(b) Histogram of total reflectance in each direction

Figure 9: Distribution of the reflective signal

$$\boldsymbol{l_2} = \boldsymbol{l_1} - 2(\boldsymbol{l_1}, \boldsymbol{n})\boldsymbol{n} \tag{5.1}$$

as well as its strength (see section 3.7).

For the convenience of depicting the direction, we transfer the rectangular coordinate system into spherical coordinate system $P(r, \theta, \varphi)$. Then we simulate the ocean surface for a period of time and collect the information of the reflective signal, which will vary in both direction and strength. After omitting the directions where the strength falls below SNR threshold, we divide the xOy plane into eight parts equally (Figure 8), and project the rest direction vectors on it. Statistic of the points (or vectors) in each part reveals the distribution of the signal direction as well as its strength. By studying the distribution, we are able to accommodate our model to a shipboard receiver, and work out the STICK-TO-THE-SAME-PATH duration.

The direction where we observe a peak in the histogram indicates the optimal direction of the maximum strength. As is shown above (Figure 9b), the weight of the histogram is calculated by summing the strength of signals that lie in the corresponding interval, and here we calculate $\sum R$ considering that the strength is proportional to the reflectance R.

We then calculate the maximum length that the signal can travel before fading out with the empirical formula (5.2):

$$Loss = 32.44 + 20(\lg distance + \lg frequency) \tag{5.2}$$

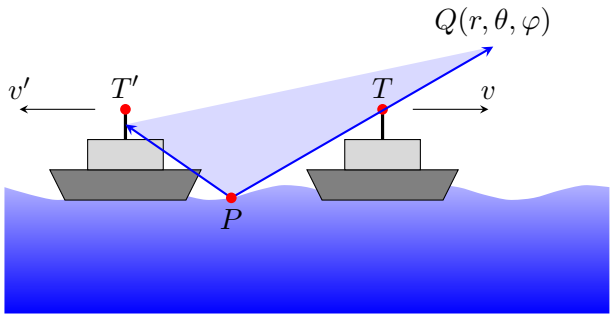

Figure 10: Diagram of the communication area

Suppose the height of the ship is H, and the signal distribution is denoted by the blue region in Figure 10. Once the shipboard receiver is no longer included in that area, we assume that the communication is at an end denoted by $Q(r, \theta, \phi)$ Then the max distance is:

$$D = \min\{H \tan\theta, r \sin\theta\} \tag{5.3}$$

6 Results of the Model

6.1 Comparison of Calm Ocean and Turbulent Ocean

Based on our model, we manage to calculate the strength of a first reflection off a calm ocean that varies with the launching angle β (Figure 11). We calculate the ratio of the reflectance of turbulent ocean to the reflectance of calm ocean (Figure 12), which equals the ratio of strength.

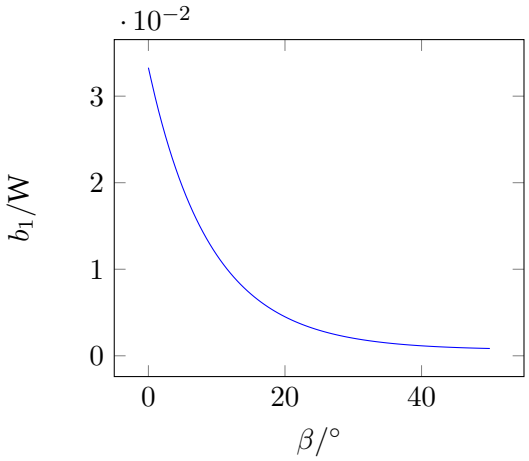

Figure 11: Relation between β and b_1

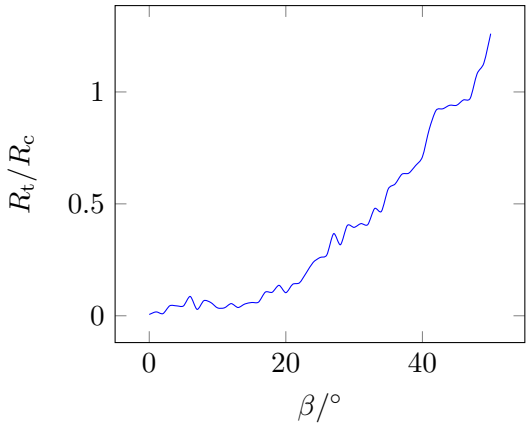

Figure 12: Ratio of the reflectance of turbulent ocean to the reflectance of turbulent ocean

6.2 Maximum number of hops

The maximum number of hops varies with the launching angle β as well (Table 3).

6.3 Reflection off different terrains

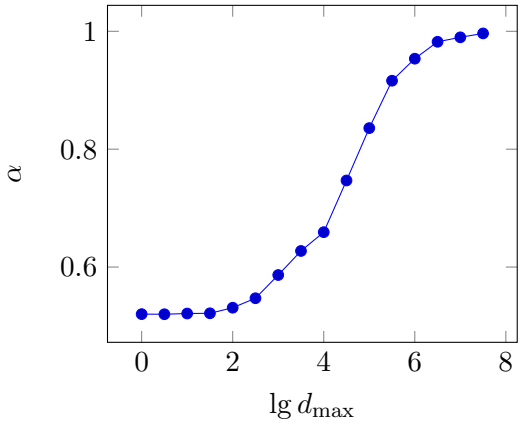

Figure 13: Relationship between α and $d_{\max}$

Table 4: α value in different terrain conditions

μ/m	σ/m	$d_{\max}$/m	α
0	0.01	100	0.997
3000	0.0	1	0.001
3000	300	100	0.537

In Table 4, μ denotes the average height of the mountains, and σ is the variance. d_{max} refers to the maximum distance of a pair of topographic inequalities. The varying of these three variables indicates the change in terrains. We also get the relationship between $alpha$ and $d_{\max}$, which is shown in Figure 13.

Table 3: Maximum Number of Hops

$\beta/°$	N_m
$[0, 11]$	3
$[12, 50]$	2

6.4 Comparison of Ocean surface and Terrain

We have calculated signal reflectance both in ocean and on land. The comparison of calm ocean and smooth terrain indicates that the reflectance of the ocean is larger than that of the smooth terrain, which means sea water tends to have a better transmission of signal than the soil and rocks do. Another evidence is that we add multiple reflections in rugged terrain, yet the ratio of strength indicates that a better reflectance lies in rugged terrain rather than in the ocean. In sum, the rugged terrain tends to have a better reflectance, though the orientation of the reflective ray is quite uncertain.

6.5 Accommodating a Shipboard receiver for Communication

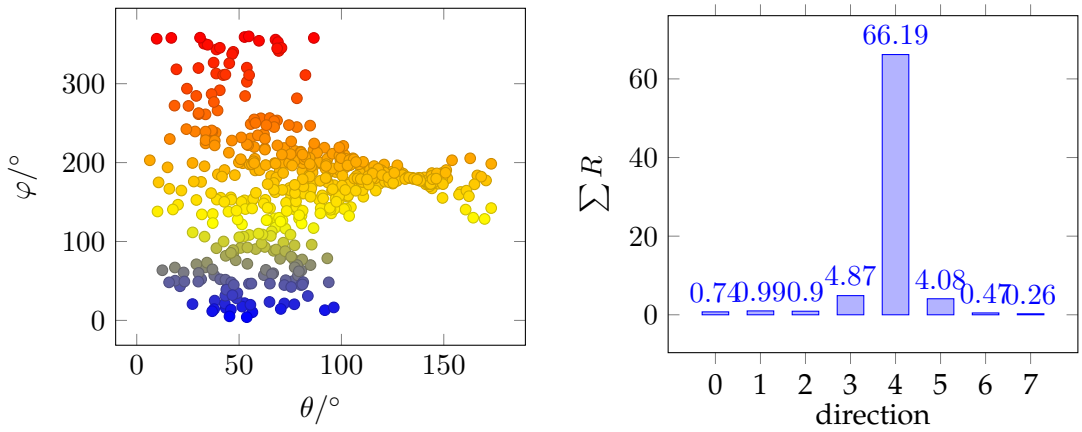

(a) Scatter graph of the distribution of θ and φ

(b) Histogram of total reflectance in each direction

Figure 14: Distribution of the reflective signal

As is shown in Figure 14a,14b, we apply the histogram analysis to develop our model. A colored point in the scatter graph represent a possible direction of the reflective signal ray, and different colors demonstrate the strength variation of the signal. By counting the number of the points that falls in each area, we can work out a histogram, which indicates the optimal direction of the heading by its peak.

Table 5: Max communication time

direction	0	1	2	3	4	5	6	7
time/s	5.186	5.135	5.501	7.556	8.508	5.825	4.893	3.904

According to the Figure 14a and Figure 8, we figure out that the duration of the communication correlates to the heading strongly, and that the optimal direction corresponds to the longest duration.

7 Evaluating & Validating the Model

7.1 Sensitivity

We analyze the sensitivity of our model through the plots we made. The Figure 11 shows how the strength of reflective signal changes with the launching angle β. We observe that the curve is monotone decreasing, and the slope increases faster when β approaches 0, which corresponds to the fact. When β is relatively small, the signal will graze the surface of ocean, which contributes to a high level of reflectance.

The fluctuation in the Figure 12 demonstrates the random behavior of our simulation of the ocean surface. From the generally increasing trend, we observe that compared with calm ocean, the reflectance on turbulent ocean increases with launching angle β. It is because when β is large, according to Fresnel Equation (3.3)(3.4), a considerable amount of the signal will dive straight into water. However, in the case of turbulent ocean, there exists some points where normal vectors have stochastic direction, thus the real incident angle maybe relatively small. Therefore, the reflectance of turbulent ocean increases.

7.2 Stability

We discuss the stability of our model especially for the model of rugged terrain. In the Figure 13, we use logarithm axis to describe the relationship of α and $d_{\max}$. First, when $d_{\max}$ becomes extremely large, which indicates the distance between two mountains tends to be relatively big. We can find the α is nearly 1 from the Figure 13, when $d_{\max}$ is a huge number. If $d_{\max}$ continues to increase, the inequality of the height ought to be omitted, therefore, the terrain is approached to a smooth one and α is approximate to 1 (see the first row of Table 4).

On the opposite, if all the mountains share a same height and the $d_{\max}$,compared with the height, becomes rather small. Now supposing a beam of signal is captured by a pair of mountains, it will remain reflecting between the mountains, because of the extremely small $d_{\max}$. This will make the pair mountains resemble a *black body* in physics. After simulating, we get $\alpha = 0.001$, which matches remarkably with the deduction above.

8 Strengths and weaknesses

8.1 Strengths

- **Application of Statistical Methods**
  The original model is a worthwhile attempt to apply the statistical tools to the HF wave propagation.
- **Detailed comparison**
  We consider the variety of ocean waves, and multiple modes of reflection in different reflecting surfaces, including calm ocean, turbulent ocean, smooth terrain and rugged terrain. The model generates the outcome that fits some certain cases well.
- **Being applicable**
  With the result of the model, ships are able to choose an optimal direction to remain in communication as long as possible.

8.2 Weaknesses

- **Computation Complexity**
  The model embodies many complex computing process, making the calculation process lengthy.
- **Propagation decay in the atmosphere is not considered in some parts**
  We fail to consider the attenuation in the atmosphere, which can be corrected by applying a loss function.
- **Some assumptions are not so convincing**
  We assume that the radio waves meet the condition of Fresnel equations, and boldly assume that the shape of mountain is not important, which is not always the case.

References

[1] X. Wang and C. Jiang, "Fading characteristics of reflex signal on hf lonospheric channels," *Chinese Journal of Radio Science*, vol. 7, no. 3, pp. 25–41, 1992.

[2] Z. Shuang, Z. Xiao-hui, and S. Chun-sheng, "Laser reflection performance from the rough sea surface with geometrical optical method," *OPTICS&OPTOELECTRONIC TECHNOLOGY*, vol. 10, no. 3, pp. 28–31, 2012.

[3] C. L. Giles and W. J. Wild, "Fresnel reflection and transmission at a planar boundary from media of equal refractive indices," *Applied Physics Letters*, vol. 40, no. 3, pp. 210–212, 1982.

[4] Z. Yun, G. Jianjing, H. Zhonghua, and H. Yanling, "Ground-based reflected gps for sea ice exploration," *CHINESE JOURNAL OF POLAR RESEARCH*, vol. 26, no. 2, pp. 262–267, 2014.

[5] R. Somaraju and J. Trumpf, "Frequency, temperature and salinity variation of the permittivity of seawater," *IEEE transactions on Antennas and Propagation*, vol. 54, no. 11, pp. 3441–3448, 2006.

[6] X. D. He, K. E. Torrance, F. X. Sillion, and D. P. Greenberg, "A comprehensive physical model for light reflection," in *ACM SIGGRAPH computer graphics*, vol. 25, pp. 175–186, ACM, 1991.

[7] Ikeuchi and Katsushi, "Lambertian reflectance," *Encyclopedia of Computer Vision*, vol. 54, 2014.

Appendices

Appendix A Details about the simulation function f

The discrete wave number k_{m_l} and k_{n_l} are defined as:

$$\begin{cases} k_{m_l} = \dfrac{2\pi m_l}{L_x} \\ k_{n_l} = \dfrac{2\pi n_l}{L_y} \end{cases} \tag{A.1}$$

We adopt the JONSWAP sea spectra to fit in the function of wave spectrum $S(k_{m_l}, k_{n_l})$:

$$S(\omega) = \alpha g \frac{1}{\omega^5} \mathrm{e}^{-\frac{5}{4}(\frac{\omega_0}{\omega})^4} \cdot \gamma^{\mathrm{e}^{-\frac{(\omega-\omega_0)^2}{2\sigma^2\omega_0^2}}} \tag{A.2}$$

g refers to the gravity acceleration, and $\omega_0 = 22\tilde{x}^{-0.33}$ is the peak frequency of the waves. $\alpha = 0.076\tilde{x}^{-0.22}$ refers to a dimensionless constant, and r is a factor that depicts how high the waves can be. Here $\tilde{x} = \dfrac{g_c x}{U_h^2}$ is a dimensionless synthesis of wind speed at the height of h and x denotes the fetch length.

Empirically, σ accords with :

$$\sigma = \begin{cases} 0.07, & \omega \le \omega_0 \\ 0.09, & \omega > \omega_0 \end{cases} \tag{A.3}$$

In the 2D cases, to consider the influence of wind, we introduce the direction factor into the JONSWAP sea spectra:

$$S(\omega, \theta) = S(\omega) G(\omega, \theta) \tag{A.4}$$

where $G(\omega, \theta)$ is called the direction distribution function of the sea spectra, and θ is the direction of view point. To simplify the calculation, we assume that the direction is unrelated to the frequency, then:

$$G(\omega, \theta) = \begin{cases} (2/\pi)\cos^2(\theta - \phi), & |\theta - \phi| < \pi/2 \\ 0, & |\theta - \phi| \ge \pi/2 \end{cases} \tag{A.5}$$

Furthermore, we consider the relation between the wave number and wave-frequency:

$$S(\omega, \theta)\, \mathrm{d}\omega\theta = S(k, \theta)\, \mathrm{d}k\, \mathrm{d}\theta = S(k_{m_l}, k_{n_l})\, \mathrm{d}k_{m_l}\, \mathrm{d}k_{n_l} \tag{A.6}$$

and

$$\omega = \sqrt{gk} \tag{A.7}$$

Eventually, for the specific pair (k_{m_l}, k_{n_l}), we have:

$$\theta = \arctan \frac{k_{n_l}}{k_{m_l}} \tag{A.8}$$

$$k = \sqrt{k_{m_l}^2 + k_{n_l}^2} \tag{A.9}$$

Appendix B Integral Formulas

Here we list the integral formulas we used to calculate α in 4.2

$$\int \arctan\frac{a}{b-x}\,\mathrm{d}x = -\frac{1}{2}a\ln\left(a^2+(b-x)^2\right) + x\arctan\frac{a}{b-x} + b\arctan\frac{b-x}{a} + C \tag{B.1}$$

$$\int \arctan\frac{a+x}{b}\,\mathrm{d}x = (a+x)\arctan\frac{a+x}{b} - \frac{1}{2}b\ln\left((a+x)^2+b^2\right) + C \tag{B.2}$$

Where C denotes arbitrary constant.